



Article

A Composite Whole-Biomass Tannin–Sucrose–Soy Protein Wood Adhesive with High Performance

Guoming Xiao ^{1,†}, Jiankun Liang ^{2,†}, Zhigang Wu ^{1,*} , Hong Lei ^{3,*} , Feiyan Gong ¹, Wen Gu ¹, Yuan Tu ¹ and De Li ¹

¹ College of Forestry, Guizhou University, Guiyang 550025, China; xgm17685381639@163.com (G.X.); 15285111783@163.com (F.G.); gwen490929@163.com (W.G.); ty0822006x@163.com (Y.T.); lide228@163.com (D.L.)

² College of Civil Engineering, Kaili University, Qiongdongnan 556011, China; dushimensheng@126.com

³ School of Chemistry and Material Engineering, Zhejiang A&F University, Hangzhou 311300, China

* Correspondence: wzhighang9@163.com (Z.W.); leihong@zafu.edu.cn (H.L.); Tel.: +86-851-8829-8397 (Z.W.)

† These authors contributed equally to this work.

Abstract: Whole-biomass adhesives are the research hotspot of wood adhesives and can improve the competitiveness of adhesives. The tannin–sucrose adhesive studied by our research group shows good bonding performance, but poor bonding stability induced by low viscosity. In this study, the tannin–sucrose adhesive was modified by isolated soybean protein (SPI), the effect of the SPI substitution ratio for tannin on the properties of the tannin–sucrose–SPI composite adhesive was investigated, and the bonding mechanism was explored using Fourier-transform infrared spectroscopy (FT-IR), thermogravimetry (TG), X-ray diffraction (XRD), and gas chromatography–mass spectroscopy (GC–MS). The results showed that: (1) when the SPI substitution ratio was above 40%, the viscosity of the composite adhesive increased significantly, which effectively avoided adhesive leakage. (2) The tannin–sucrose–SPI composite adhesive displayed high bonding performance and water resistance. (3) The FTIR and GC–MS results revealed that the curing mechanism of the tannin–sucrose–SPI adhesive was very complicated, but it was certain that the conversion of sucrose into furan compounds, especially 5-hydroxymethylfurfural (5-HMF), was the core of the cross-linking reaction of the adhesive when elevating temperature. (4) The macromolecules and high reactivity of SPI compensated for the shortage of high temperature required for the conversion of sucrose into furanic cross-linkers so that the tannin–sucrose–SPI adhesive experienced an efficient curing reaction at a low temperature, and the reaction degree and thermal stability of the curing product increased.

Keywords: tannin; sucrose; SPI; cross-linking; whole-biomass wood adhesive; plywood



Citation: Xiao, G.; Liang, J.; Wu, Z.; Lei, H.; Gong, F.; Gu, W.; Tu, Y.; Li, D. A Composite Whole-Biomass Tannin–Sucrose–Soy Protein Wood Adhesive with High Performance. *Forests* **2023**, *14*, 1250. <https://doi.org/10.3390/f14061250>

Academic Editor: Nadir Ayrimis

Received: 19 May 2023

Revised: 11 June 2023

Accepted: 14 June 2023

Published: 15 June 2023



Copyright: © 2023 by the authors. Licensee MDPI, Basel, Switzerland. This article is an open access article distributed under the terms and conditions of the Creative Commons Attribution (CC BY) license (<https://creativecommons.org/licenses/by/4.0/>).

1. Introduction

With the increasing shortage of non-renewable resources and the continuous improvement of people's awareness of environmental protection, biomass adhesives have become the development goal of wood adhesives [1–4]. In recent years, biomass adhesives have been increasingly reported, mainly focusing on protein adhesives [5–7], tannin adhesives [8,9], lignin adhesives [10,11], and starch adhesives [12–14]. Wood adhesives prepared with tannin over a long period of time have been successfully applied to industrial production in some countries. Tannin has a similar chemical structure with phenol and can be divided into hydrolyzed tannin and condensed tannin. Condensed tannin has high reactivity (mainly determined by the A ring) and was often used for the preparation of wood adhesive. The structural units of condensed tannin can be divided into the resorcinol A-ring type and the phloroglucinol A-ring type according to the absence/presence of hydroxyl groups in the C₅ position of the A ring [15–17].

Condensed tannin has been applied in wood adhesives mainly for two purposes: first, it is used to modify formaldehyde-based wood adhesives to reduce formaldehyde release

in resin [18], which, however, will also reduce the water resistance and storage stability of resin. Second, it is directly used to prepare tannin-based wood adhesives. Resorcinol A-ring *Acacia mearnsii* and quebracho tannin adhesives were first used in research, which can be used alone or blended with phenol-formaldehyde resin or urea-formaldehyde resin to prepare reinforced adhesives and are widely used in particleboard, plywood, laminated wood, etc. [19,20]. Phloroglucinol A-ring tannin can also be used to prepare room-temperature curing-type adhesives because of its high reactivity, but it is not as widely used as resorcinol A-ring tannin. Besides blending with conventional phenol-formaldehyde resin or urea-formaldehyde resin, tannin can be used to replace part of resorcinol in phenol-resorcinol-formaldehyde resin or resorcinol-formaldehyde resin [21]. Formaldehyde or formaldehyde resin is the most commonly used cross-linker in tannin-based adhesives; however, formaldehyde still poses a potential threat to the environment. In particular, the biggest threat is related to adverse human health effects, including cancer [22,23].

Xi et al. [24] performed oxidative cleavage of glucose with sodium periodate to generate various nonvolatile aldehydes, all of which could react with tannin, thus realizing the cross-linking and curing of tannin. Li et al. [25] simulated the bonding mechanism of shellfish mucilage protein, and made tannin, the B-ring structure of which could easily generate *o*-quinone, react with polyethyleneimine to prepare tannin-based adhesives for the wood industry, and the plywood fabricated in this way had high bonding strength and excellent water resistance. On this basis, Xi successfully prepared high-performance tannin adhesives with hexamethylene diamine as the cross-linker [8]. Different to the reaction mechanism of traditional tannin-based wood adhesives, the above studies provide a new idea for the preparation of tannin-based wood adhesives. In addition, the cured products of tannin adhesives with epoxy resin, polyamide, and isocyanate were denser and more compact, and the bonding performance and water resistance were greatly improved [26–28]. However, these cross-linkers, which are from the petroleum industry, reduce the advantages of biomass adhesives.

In the previous work [29], our research group successfully prepared a type of whole-biomass adhesive with good bonding performance from *Myrica rubra* tannin and sucrose. The bonding mechanism was mainly that sucrose was converted into 5-hydroxymethylfurfural (5-HMF) and then cross-linked with tannin, but the adhesive had poor bonding stability due to its low viscosity. Isolated soybean protein (SPI) was characterized by a large molecular weight, long molecular chains, and high reactivity [30–33]. In this study, the tannin–sucrose adhesive was modified with SPI, which could not only improve the viscosity of the adhesive, but also exert a reinforcing and toughening effect on the adhesive.

2. Materials and Methods

2.1. Materials

Myrica rubra Tannin, 160-mesh, industrial grade, was produced by Guangxi Wuming Tannin Extract Plant Co., Ltd. (Nanning, China). Sucrose with a purity of 99.0% and sodium dodecyl benzene sulfonate with a purity of 90.0% were purchased from Chengdu Jinshan Chemical Reagent Co., Ltd. Soy Protein Isolate (SPI) with a purity of 90% was bought from Shandong Gushen Biotechnology Group Co., Ltd. (Dezhou, China). *Populus* spp. veneer with a moisture content of 8%–10% and a size of 400 mm × 400 mm × 1.5 mm, was from Shuyang, Jiangsu.

2.2. Preparation of Tannin–Sucrose–SPI Adhesive

At room temperature, a certain amount of distilled water was added into a round-bottomed three-neck flask, the temperature was raised to 50–55 °C in a water bath, a certain amount of sucrose was added and fully dissolved, and a certain amount of tannin was added in batches and fully stirred for 30 min. The temperature was elevated to 60 °C, a certain amount of SPI was gradually added, and the mixture was fully stirred for 50 min, and then cooled. As seen in Table 1, different tannin–sucrose–SPI composite adhesives were prepared by changing the substitution ratio of SPI for tannin.

Table 1. The formulation of tannin–sucrose–soy protein wood adhesive.

Substitution Ratio/%	Tannin/g	SPI/g	Sucrose/g	Water/g	SDBS/g
0%	30	—	20	33.3	1.5
5%	28.5	1.5	20	33.3	1.5
10%	27.0	3.0	20	33.3	1.5
15%	25.5	4.5	20	33.3	1.5
20%	24.0	6.0	20	33.3	1.5
30%	21.0	9.0	20	33.3	1.5
40%	18.0	12.0	20	33.3	1.5
50%	15.0	15.0	20	33.3	1.5
60%	12.0	18.0	20	33.3	1.5

2.3. Preparation of Plywood and the Test of Bonding Strength

After the adhesive was coated on the veneer with a single-sided adhesive consumption of 160 g/m², the assembled plywood was placed at room temperature for 20 min, and then the three-layer plywood with a width of 400 mm × 400 mm was exposed to single-layer hot press unit (XLB type) at Shanghai Rubber Machinery Plant and pressed with a pressure of hot-pressing temperature of 200 °C and 220 °C, hot-pressing pressure of 1.2 MPa, and hot-pressing time of 1.2 min/mm. According to the national standard GB/T 17657-2022 [34], the bonding strength of plywood in warm water and boiling water was tested, respectively. The reported strength is the mean of 12 specimens.

2.4. Test of Insoluble Substance Rate in Cured Adhesives

The adhesive was wrapped with a piece of tin foil paper, and then absolutely dried in a constant temperature ventilated drying oven at 60–70 °C. The subsequent test and calculations of insoluble substance rate were carried out according to the previous work [29]: The adhesive was placed in the tin foil, and then put it in a constant temperature ventilated drying oven at 60–70 °C until the weight was constant. Then, it was put into the mill grinding through a 200-mesh sieve. Overall, 2.0 g adhesive powders were taken out and dried in a thermostatic ventilation drying oven at 220 °C for 12 min, and then it was put into the mill grinding through a 200-mesh sieve again to obtain cured adhesive powder. The cured adhesive powders were soaked in water at 63 °C for 6 h, and dried in a thermostatic drying oven at 120 °C, the insoluble substance content was obtained according to the change in weight.

2.5. Differential Scanning Calorimetry (DSC)

The curing performance of the adhesive was measured by DSC 204 F1 differential scanning calorimeter produced by Netzsch Company in Germany under N₂ protection, with a temperature range of 30–350 °C, and a heating rate of 10 °C/min.

2.6. Thermogravimetry (TG)

The thermal stability of the adhesive was determined using a TG 209 F3 thermogravimetric analyzer produced by Netzsch Company in Germany under N₂ protection, temperature range of 30–600 °C with a heating rate of 10 °C/min.

2.7. X-ray Diffraction (XRD)

The crystallization properties of the curing product of the adhesive were tested using a TTR X-ray diffractometer produced by RIGAKU, Japan. Parameters were Cu target ($\lambda = 0.154060$ nm), 2θ scanning range of 5–90°, step size of 0.02°, scanning rate of 5°/min, tube current of 120 mA, and tube voltage of 40 kV.

2.8. Fourier Transform Infrared Spectroscopy (FT-IR)

A Varian 1000 (Varian, PaloAlto, CA, USA) infrared spectrometer was used to analyze the structural characteristics of the cured adhesive. Adhesive powder was mixed with KBr

to prepare a pellet. The parameters were a wave number range of 400–4000 cm^{-1} with 32 scans, and a resolution of 4 cm^{-1} .

2.9. Gas Chromatography–Mass Spectroscopy (GC–MS)

The structural characteristics of the curing product of the adhesive were analyzed using a 7890A-5975C (Agilent Technology Co., Ltd., Santa Clara, CA, USA) GC-mass spectrometer.

Chromatographic conditions: the chromatographic column was HP-17MS (30.0 m \times 250 μm , 0.25 μm); the initial temperature of the chromatographic column was kept at 45 $^{\circ}\text{C}$ for 4 min, and then it was raised to 280 $^{\circ}\text{C}$ at the rate of 13 $^{\circ}\text{C}/\text{min}$, which was kept for 15 min; the temperature of the gasification chamber was 250 $^{\circ}\text{C}$; the transmission line temperature was 280 $^{\circ}\text{C}$; the carrier gas was He; the flow rate of the carrier gas was 1.0 mL/min; the split ratio was 20:1; the sample injection volume was 1 μL .

MS conditions: EI source; electron energy of 70 eV; ion source temperature of 230 $^{\circ}\text{C}$; quadrupole temperature of 150 $^{\circ}\text{C}$; scan mode of Scan; scanning mass range of 15–500 u.

Qualitative and quantitative methods: the detected components were qualitatively determined by NIST11, retention time, and retention index of MS database; the column loss peak was deducted from the database. In addition, the components were quantified through the area normalization method, that is, the percentage of the peak area of the identified components in the area sum of all the identified component was taken as the quantification result.

3. Results and Discussion

3.1. Effect of Substitution Ratio on the Properties and Bonding Performance of the Composite Adhesive

Figure 1 shows the effect of different substitution ratios on bonding performance of plywood in warm water of tannin–sucrose–SPI composite adhesives at hot-pressing temperatures of 200 $^{\circ}\text{C}$ and 220 $^{\circ}\text{C}$. Water resistance strength and wood failure rate can reflect the bonding quality and reliability of wood-based panels. At hot-pressing temperature of 200 $^{\circ}\text{C}$, the plywood prepared by the tannin–sucrose adhesive did not have warm water resistance. The key to the good bonding performance of the tannin–sucrose adhesive lies in the cross-linking reaction with tannin after sucrose conversion into 5-HMF [29]. The increase in hot-pressing temperature is beneficial to the formation of 5-HMF. Therefore, when the hot-pressing temperature rose to 220 $^{\circ}\text{C}$, the plywood prepared with the tannin–sucrose adhesive could obtain the bonding strength of 1.22 MPa. It could meet the strength requirements (≥ 0.7 MPa) in GB/T 17657-2022 (Class II), but the 5% wood failure rate indicated a low bonding reliability. When the hot-pressing temperature was 200 $^{\circ}\text{C}$, the wet bonding strength of plywood prepared with the tannin–sucrose–SPI composite adhesive increased significantly. When the substitution ratio was 5%–40%, the bonding strength increased from 0.72 MPa to 1.85 MPa, and the wood failure rate grew from 0% to 90%, indicating that SPI could significantly improve the bonding strength and bonding reliability of the composite adhesive. At the substitution ratio of 50%–60%, the bonding strength decreased slightly, but the bonding reliability clearly decreased.

At a substitution ratio of 15% and a hot-pressing temperature of 200 $^{\circ}\text{C}$, the warm water bonding strength with the tannin–sucrose–SPI adhesive was 1.23 MPa with a wood failure rate of 20%. In this case, the bonding strength of the composite adhesive was basically the same as that of tannin–sucrose at 220 $^{\circ}\text{C}$, but the bonding reliability of the former was higher. Despite the slightly low conversion rate of 5-HMF at the hot-pressing temperature of 200 $^{\circ}\text{C}$, the insufficient generation of 5-HMF could be compensated by the introduction of SPI. In other words, the tannin–sucrose–SPI composite adhesive could acquire ideal bonding performance at a low hot-pressing temperature. The effect of different substitution ratios on bonding performance of plywood in boiling water of the composite adhesive is displayed in Figure 2. Similarly, the change trend of the influence of the substitution ratio on the boiling water bonding strength of the adhesive was basically consistent with that on the warm water. Therefore, the tannin–sucrose–SPI composite

adhesive exhibited excellent bonding strength and bonding stability, and the prepared plywood could meet the strength requirements of Class II and Class I plywood in GB/T 17657-2013; thus, it had great application prospects.

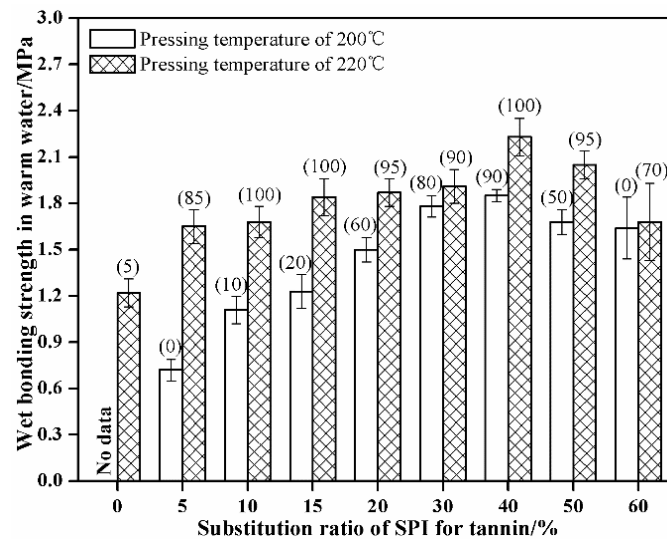


Figure 1. Effect of substitution ratio on warm water bonding performance of the composite adhesive. Note: The number in brackets is the wood failure rate.

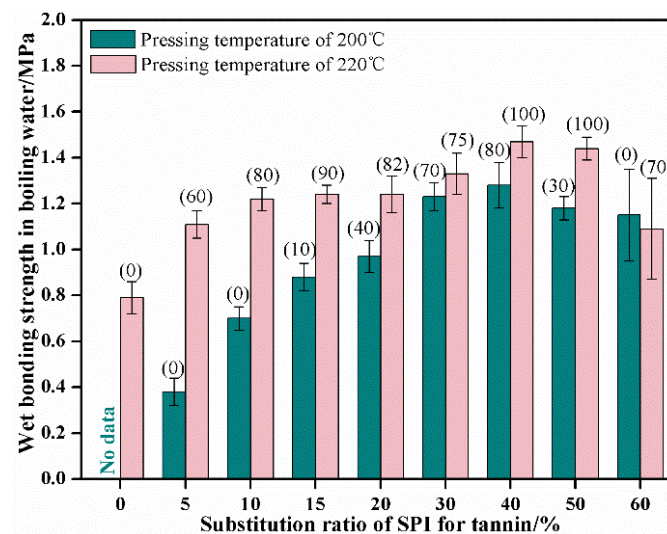


Figure 2. Effect of substitution ratio on boiling water bonding performance of the composite adhesive. Note: The number in brackets is the wood failure rate.

The effects of the substitution ratio of tannin to SPI on the viscosity and pH of the composite adhesive are shown in Figure 3. The polyphenol compounds contained in tannin tended to ionize H⁺ in aqueous solution to form a relatively stable benzoquinone structure, which made the aqueous solution acidic [27,28]. The content of basic amino acids in SPI was relatively large so that the aqueous solution of SPI was alkaline (about 8.2). When the substitution ratio was 5%–50%, the pH of the adhesive increased slowly from 5.9 to 6.9. When the substitution ratio was 60%, the pH was 7. The previous research results show that a weak acid environment is beneficial to the cross-linking and curing of the tannin–sucrose adhesive system [29]; thus, the substitution ratio of SPI should not exceed 60%.

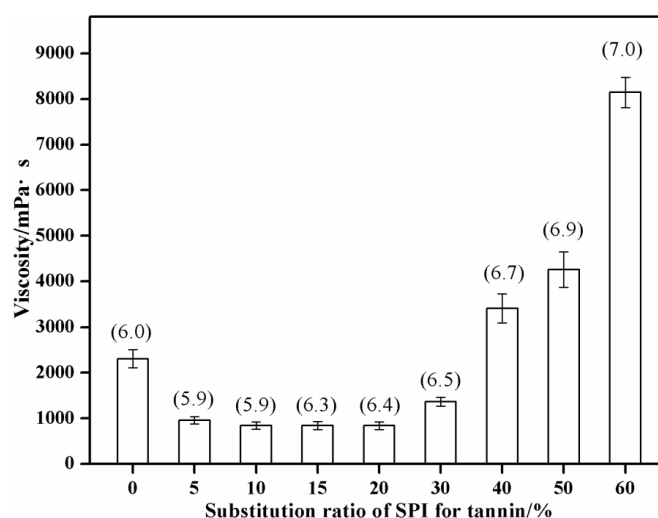


Figure 3. Effect of substitution ratio on the viscosity and pH of the composite adhesive. Note: The number in brackets is the pH value.

With the gradual increase in SPI, the viscosity of the adhesive system decreased slowly at first and then increased sharply. This is because: (1) the pH gradually decreases until it is near the isoelectric point of the soy protein, and the protein exists in the form of aggregates due to the decrease in charges and the enhancement of hydrophobic interaction, accompanied by the smallest electrostatic repulsion between the protein and worsening dissolubility, thus reducing the viscosity [35]. (2) Soy protein has non-Newtonian hydrodynamic behavior. When the protein concentration is lower than the critical concentration, the intermolecular distance of protein becomes farther because of water, the acting force decreases, and the viscosity decreases [36]. As the amount of SPI increases and reaches the critical concentration, the expanded protein molecules do not have enough space to disperse, the molecules are cross-linked, the intermolecular force is great, and the viscosity increases rapidly. (3) Tannin molecules contain many phenol hydroxyl groups with a large area of hydrophobic association with protein, which can bind to SPI through the combined action of multi-point hydrophobic bonds and hydrogen bonds [37]. In addition, the viscosity of the system can also be increased by the tanning effect between tannin and protein.

It could be known by combining Figures 1–3 that the viscosity of the adhesive without SPI was low (about 2000 mPa·s), and it tended to excessively permeate the wood surface, leading to a lack of adhesive on the bonding surface and low bonding strength and wood failure of the tannin–sucrose adhesive. At the substitution ratio of 60%, the viscosity of the tannin–sucrose–SPI composite adhesive was too large (8142.2 mPa·s), which resulted in the poor liquidity of the adhesive. Consequently, adhesive spreading was difficult, and the adhesive was unevenly distributed during the hot pressing, which led to the decline in bonding strength and wood failure. Hence, when the substitution ratio was 40% and 50%, the viscosity of 3412.8 mPa·s and 4263.6 mPa·s was relatively suitable for the tannin–sucrose–SPI composite adhesive.

3.2. Curing Performance Analysis

Figure 4 shows the test results of insoluble matter in the cured product of tannin–sucrose adhesive and tannin–sucrose–SPI adhesive at different curing temperatures. The curing temperature of the tannin–sucrose adhesive grew from 190 °C to 220 °C, and the insoluble ratio increased from 15% to 31%, with an increase of 16%, indicating that the tannin–sucrose adhesive needed a higher curing temperature, which was related to the high temperature needed by the conversion of sucrose to form furanic cross-linkers. However, the too-high hot-pressing temperature would result in the deformation and discoloring of the prepared wood-based panel and consume a greater amount of energy.

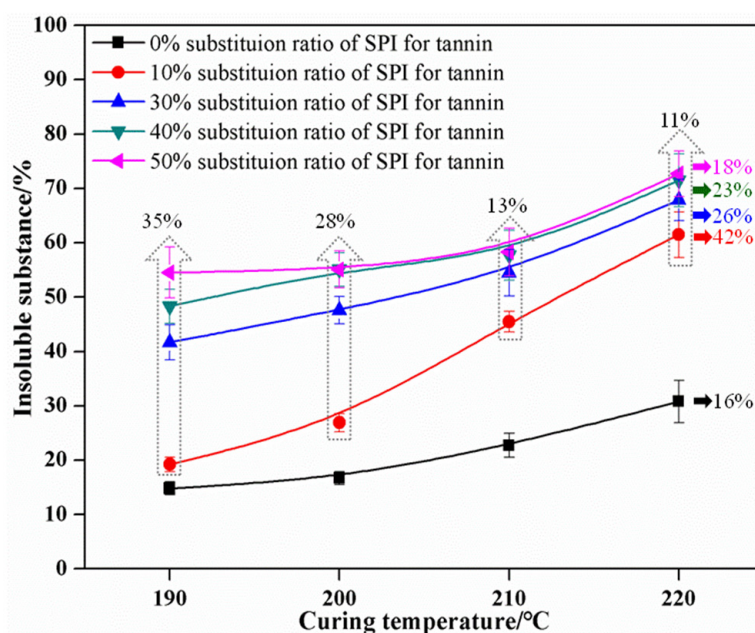


Figure 4. Effects of curing temperature on insoluble content in the cured adhesive.

By horizontally comparing the results in Figure 4, it could be known that the insoluble ratio in the cured tannin–sucrose–SPI adhesive at 190 °C with substitution ratios of 10%, 30%, 40%, and 50% was 19%, 42%, 48%, and 55%, respectively. When the curing temperature was raised to 220 °C, the insoluble matter content in the cured product increased to 61%, 68%, 71%, and 73%, with an increase of 42%, 26%, 23%, and 18%, respectively. The cross-linking degree and cross-linking density of the cured product varied with the substitution ratio too. As the adhesive curing temperature grew from 190 °C to 220 °C, the insoluble content in the cured product reached the maximum increase amplitude at the substitution ratio of 10%, indicating the high cross-linking degree and cross-linking density of the cured adhesive. With the increase in the substitution ratio, the increase amplitude of the insoluble content in the cured adhesive gradually declined. After SPI was introduced in the tannin–sucrose composite adhesive, the insoluble content in the curing product was elevated significantly, manifesting that SPI experienced a cross-linking reaction with the tannin–sucrose system, accompanied by the large cohesion strength and high compactness in the cured adhesive and the bonding strength and water resistance was enhanced significantly.

It could be known by longitudinally comparing the results in Figure 4 that as the substitution ratio grew from 10% to 50%, the insoluble content in the curing product increased by 35%, 28%, 13%, and 11% at curing temperatures of 190 °C, 200 °C, 210 °C, and 220 °C, respectively. Very obviously, the curing efficiency was higher for the tannin–sucrose–SPI composite adhesive; in particular, high curing efficiency could be achieved at 190 °C, namely, SPI could facilitate the curing reaction at a low temperature.

Figure 5 shows the DSC results of the tannin–sucrose adhesive and the tannin–sucrose–SPI adhesive. The tannin–sucrose adhesive could be cured effectively at 204 °C. The SPI adhesive without a cross-linker showed no obvious exothermal reaction [38], whereas that of the tannin–sucrose–SPI adhesive was 192 °C. DSC test results also further proved that the tannin–sucrose–SPI adhesive could be cured at a low temperature.

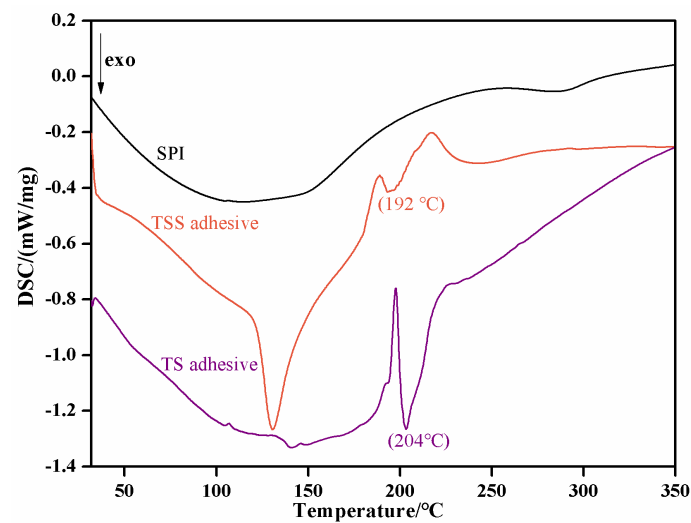


Figure 5. DSC curves of tannin-sucrose adhesive (TS) and tannin-sucrose-SPI adhesive (TSS).

To sum up, the macromolecules and high reactivity of SPI compensated for the high temperature needed by the conversion of sucrose into furanic cross-linkers so as to facilitate the efficient curing reaction of the tannin-sucrose-SPI adhesive at a low temperature.

3.3. Thermal Stability Analysis

Previous work shows that the maximum thermal weight loss on the TG-DTG curve of the tannin-sucrose adhesive mainly occurs around 300 °C, which is mainly ascribed to the thermal decomposition of sucrose degradation products (especially furanic compounds) and its cross-linked products with tannin [29]. The TG-DTG curves of the tannin-sucrose-SPI adhesive and the tannin-sucrose adhesive are displayed in Figures 6 and 7. The greatest difference between the two was that the former had two primary thermal decomposition peaks near 210 °C and 300 °C, which were attributed to the thermal decomposition of the cross-linked products of SPI with tannin and sucrose and sucrose degradation products with SPI and tannin.

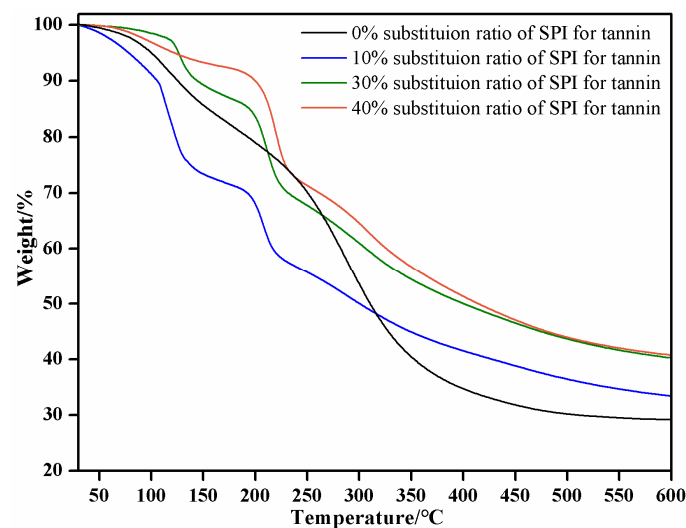


Figure 6. TG results of cured tannin-sucrose-SPI adhesive at different SPI substitution ratios.

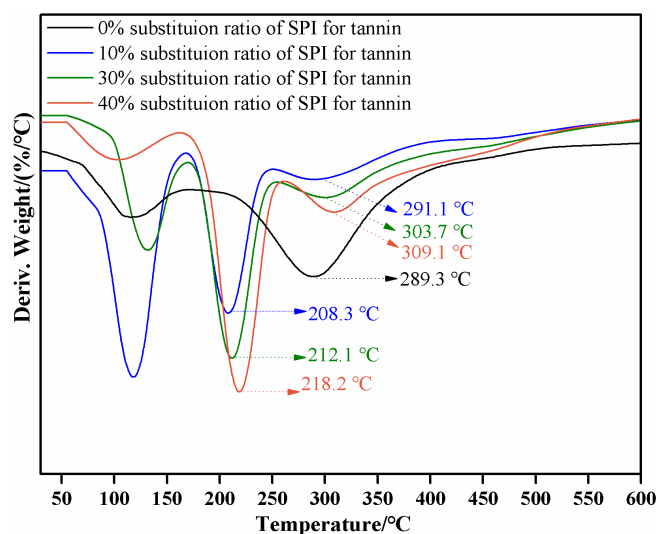


Figure 7. DTG results of cured tannin–sucrose–SPI adhesive at different SPI substitution ratios.

The similar TG–DTG curves reflecting the similar thermal analysis course of the adhesives with different SPI substitution ratios. At the SPI substitution ratios of 10%, 30%, and 40%, the first primary thermal decomposition temperature was 208.3 °C, 212.1 °C, and 218.2 °C, respectively, and the second was 291.1 °C, 303.7 °C, and 309.1 °C, respectively. With the increase in the SPI substitution ratio, the two thermal decomposition temperatures gradually increased, further proving that SPI participated in the cross-linking reaction of the system and also reflecting that the reaction degree and thermal stability of cross-linked products increased.

3.4. Crystallization Property Analysis of Cured Adhesive

As shown in Figure 8, SPI had two crystalline regions at diffraction angles nearby 9° and 20°, which were α -helix and β -folded crystalline region of protein [39]. Tannin–sucrose–SPI adhesive and tannin–sucrose adhesive both had crystallization peaks at 22.6°, which was the diffraction peak of the cross-linked product of tannin and sucrose. The tannin–sucrose–SPI adhesive had new crystallization peaks at 31.8° and 33.3°, which were the diffraction peaks of the cross-linked products of SPI with tannin and sucrose. Crystallinity reflects the degree of ordered arrangement of molecules, which can show the degree of cross-linking reaction of the adhesive to some extent. The crystallinity of the cured the tannin–sucrose adhesive at 200 °C was only 4.7%, indicating that the cross-linking reaction was insufficient and the cross-linking density of the curried adhesive was low. Similarly, a new crystallization peak was formed, and the crystallinity also increased after adding SPI, manifesting that the cross-linking degree increased, and the crystallinity was further improved by increasing the substitution ratio and curing temperature. However, the crystallinity at 33.3° decreased somehow when the curing temperature was raised to 220 °C, because although high temperature was helpful to further improve the conversion of furanic compounds, the cross-linking degree and density of tannin and SPI were too high, which would reduce the crystallinity on the contrary [30,31,40]. In addition, the crystallinity of cross-linked products would also be reduced due to their decomposition at high curing temperature. Thus, it could be seen that the increasing SPI substitution ratio was more beneficial for the overall performance improvement of the adhesive than elevating the curing temperature.

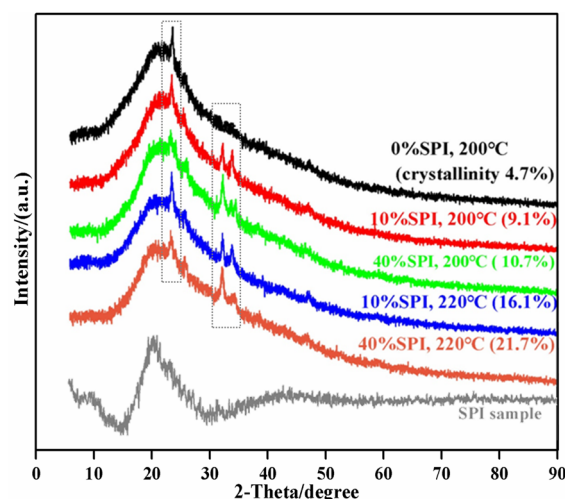


Figure 8. XRD curves of cured tannin–sucrose–SPI adhesive at different substitution ratios.

3.5. Bonding Mechanism Analysis of the Tannin–Sucrose–SPI Adhesive

Figure 9 exhibits the FT-IR results of the curing products of the tannin–sucrose adhesive, tannin–sucrose–SPI adhesive and SPI sample. The peaks at 1518.3 and 1455.3 cm^{-1} were the skeleton carbon absorption peaks on tannin benzene ring, and 843.1 cm^{-1} was the C-H bending vibration peak of tannin aromatic ring. 992.3 cm^{-1} was the hydroxymethyl absorption peak of sucrose, 925.0 cm^{-1} was the pyranose ring of sucrose, and 1048.5 cm^{-1} was the ether bond of the sucrose [41–43]. Part of the sucrose depolymerized and converted to furan compounds (764.7 cm^{-1} was the furan ring CH=CH) and then reacted with tannin to form an ether bond (1123.1 cm^{-1}).

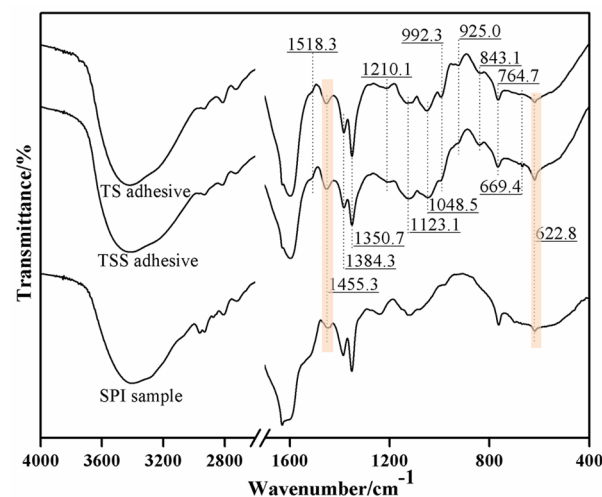


Figure 9. FT-IR curves of cured tannin–sucrose adhesive (TS), tannin–sucrose–SPI adhesive (TSS).

The absorption peaks of the tannin–sucrose–SPI adhesive almost disappeared at 992.3 and 925.0 cm^{-1} , which indicated more depolymerized sucrose and converted into furan compounds, which participated in the curing reaction of the adhesive, resulting in a significant increase in the peak at 1123.1 cm^{-1} . The new 669.4 cm^{-1} peak was the N-H out-of-plane bending vibration peak, while the vibration peaks at 622.8 and 1455.3 cm^{-1} increased in intensity, which was related to the C-N stretching vibration [32,33], thus indicating a chemical interaction between tannin and soy protein.

It is difficult to determine the detailed curing mechanism only by FT-IR, so the reaction mechanism of the tannin–sucrose–SPI adhesive was further analyzed by GC–MS. Figure 10 displays the GC–MS result of the cured product of the tannin–sucrose–SPI adhesive, and the corresponding structures matched are summarized in Table 2.

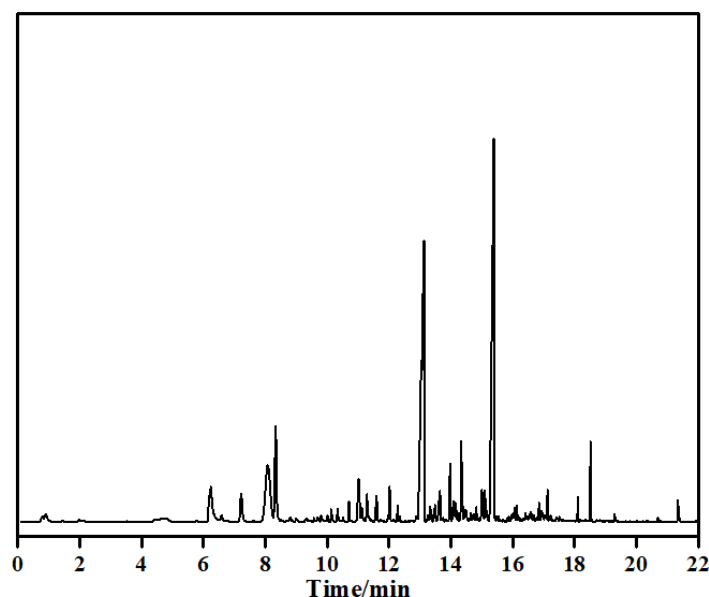
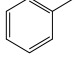
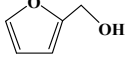
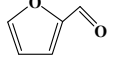
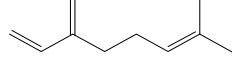
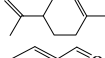
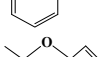
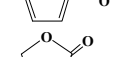
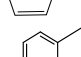
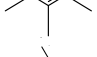
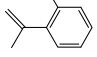
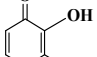
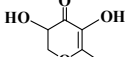
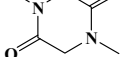
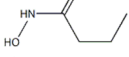
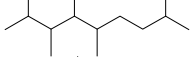
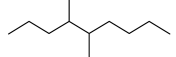
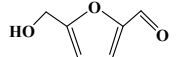
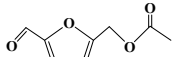
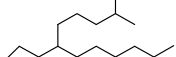
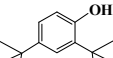
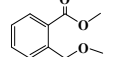

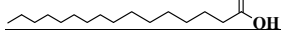


Figure 10. GC-MS curve of cured tannin-sucrose-SPI adhesive.

It could be seen from Table 2 that the corresponding structure of NO.17 was 5-HMF with relatively high content, which was converted from sucrose, indicating that the alienation of sucrose into 5-HMF was an important reaction in the curing process of the adhesive, which coincided with the infrared test results. Two high-activity functional groups—aldehyde and hydroxymethyl—were contained on the molecule of 5-HMF, which could experience such reactions as esterification, condensation, and oxidation [44,45]. As early as the last century, it was found by scholars that the bonding strength of melamine-formaldehyde resin and the toughness of the cured product could be effectively improved by introducing sucrose into it. It was then believed that sucrose participated in co-polycondensation in some ways, and this specific substance was proved to be 5-HMF [7]. Formaldehyde and formaldehyde-based resin are active curing agents of biomass tannin adhesive and soy protein adhesive, and a large amount of hydroxymethyl contained in them can cross-link with active groups such as hydroxyl, carboxyl, and amino in tannin and protein molecules. 5-HMF and formaldehyde are similar in structure, thus also being subjected to the above reaction. Moreover, compared with formaldehyde, 5-HMF derives from biomass sugar, which is more environmentally friendly with a wide range of raw materials. Moreover, the co-polycondensation reaction is easy to form a branched structure, which is more conducive to curing to form an insoluble spatial network structure.

NO.2, NO.3, NO.7, NO.8, NO.17, NO.18, and NO.22 exhibited a large number of furan structures in the cured adhesive, manifesting that 5-HMF exerted a significant cross-linking effect during the adhesive curing process. The structures of NO.13 and NO.14 contained nitrogen-containing heterocycles, indicating that nitrogen-containing compounds were another main component of the cured adhesive, which were attributed to the characteristic reaction between 5-HMF and SPI. Specifically, NO.14 contained C-N and C=N bonds, reflecting that Schiff base reaction occurred between aldehyde group of 5-HMF and amide of soy protein. Such a reaction indicated that 5-HMF could effectively cross-link with SPI, thereby considerably improving the bonding strength and water resistance. NO.18 contained the C-O-C bond, manifesting that the cross-linked product between 5-HMF and soy protein still existed in the form of a dimethylene ether bridge.

Table 2. The main peaks of GC–MS and their chemical structure assignment.

NO.	TR/min	Compound	MW	CAS	Molecular Formula	Chemical Structure
1	0.9	Toluene	92.1	000108-88-3	C ₇ H ₈	
2	6.19	Furfural alcohol	98.0	000098-00-0	C ₅ H ₆ O ₂	
3	6.24	Furfuraldehyde	96.0	000098-01-1	C ₅ H ₄ O	
4	7.22	Myrcene	136.1	000123-35-3	C ₁₀ H ₁₆	
5	8.33	Dipentene-	136.1	005989-27-5	C ₁₀ H ₁₆	
6	9.58	Benzaldehyde	106.0	000100-52-7	C ₇ H ₆ O	
7	9.8	5-Methyl-2-furaldehyde	110.0	000620-02-0	C ₆ H ₆ O ₂	
8	1.13	2(5H)-Furanone	84.0	000497-23-4	C ₄ H ₄ O ₂	
9	11.13	Benzene, 1,2,3,4-tetramethyl-	134.1	000488-23-3	C ₁₀ H ₁₄	
10	11.28	1-isopropyl-2-methylbenzene	134.1	000527-84-4	C ₁₀ H ₁₄	
11	12.89	3-Hydroxy-2-methyl-4-pyrone	126.0	000118-71-8	C ₆ H ₆ O ₃	
12	13.12	2,3-dihydro-3,5-dihydroxy-6-me	144.0	028564-83-2	C ₆ H ₈ O ₄	
13	13.64	2,5-Piperazinedione,1,4-dimethyl-	142.0	005076-82-4	C ₆ H ₁₀ N ₂ O ₂	
14	13.98	Butanimidamide, N-hydroxy-	102.1	027620-10-6	C ₄ H ₁₀ N ₂ O	
15	14.34	2,3,5,8-Tetramethyldecane	366.4	192823-15-7	C ₁₄ H ₃₀	
16	14.64	Isobornyl methacrylate	226.3	055045-08-4	C ₁₁ H ₂₄	
17	15.38	5-Hydroxymethylfurfural	126.0	000067-47-0	C ₆ H ₆ O ₃	
18	16.14	5-Acetoxyethyl-2-furaldehyde	168.0	010551-58-3	C ₈ H ₈ O ₄	
19	16.92	Dodecane, 2-methyl-6-propyl-	226.3	055045-08-4	C ₁₄ H ₃₄	
20	17.12	Phenol,2,4-bis(1,1-dimethylethyl)-	206.2	000096-76-4	C ₁₄ H ₂₂ O	
21	18.11	Dimethyl phthalate	194.1	000131-11-3	C ₁₀ H ₁₀ O ₄	
22	18.52	Cedrol	222.2	000077-53-2	C ₁₅ H ₂₆ O	
23	21.34	Hexadecanoic acid	256.3	000057-10-3	C ₁₆ H ₃₂ O ₂	

The corresponding structures of NO.20 and NO.21 showed that tannin participated in the polycondensation reaction of the adhesive well, especially the latter structure presented an esterification reaction between the phenol ring structure of tannin and SPI carboxyl groups. NO.22 contained overlapping rings, which mainly derived from the DA addition reaction between furan rings or between furan rings and the double bond structure in tannin or protein [44], which further increased reaction sites of the polycondensation, expanded the spatial network structure of the cured adhesive, and exerted a great effect on improving the toughness and bonding strength of tannin–sucrose–SPI adhesive.

Residence time of GC–MS and structural analysis showed that the curing reaction was complicated, and there were other complicated isomerization reactions in the system, which all contributed to the improvement of bonding strength to varying degrees.

Based on the above analysis, the curing mechanism of the tannin–sucrose–SPI adhesive was very complicated. It was certain, however, that the conversion of sucrose into furan compounds, especially 5-HMF, was the core of the cross-linking reaction of the tannin–sucrose–SPI adhesive when elevating temperature (Figure 11). The adhesive curing product was composed of 5-HMF, furan compounds, Schiff base (reaction product of 5-HMF and SPI), esterification products of 5-HMF with tannin and protein, etc.

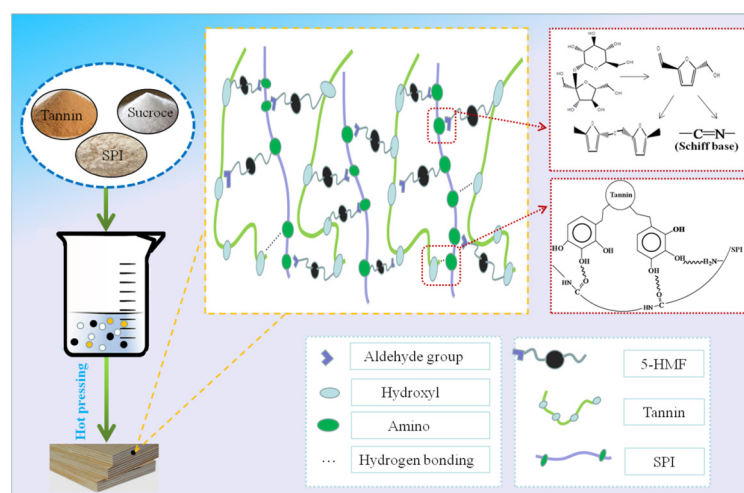


Figure 11. Schematic diagram of bonding mechanisms for tannin–sucrose–SPI wood adhesive.

During the curing process of the tannin–sucrose adhesive, 5-HMF reacted with C₆ and C₈ positions of the tannin A ring [29], but with the increase in the degree of reaction between them, the rigidity of the curing adhesive increased due to the increasing cross-linking density, and the cured adhesive layer was prone to cracking, which finally led to the decrease in water resistance and bonding stability. For the tannin–sucrose–SPI adhesive, long-chain SPI molecules were interspersed into the system to improve the overall flexibility of the adhesive, and the cross-linking structure and cross-linking density were further enhanced. The bonding layer of cured adhesive formed a dense and compact structure, and meanwhile, there was a better elastic contact and regular arrangement in the cured adhesive, which was more conducive to waterproof and the water resistance of the adhesive [7,36,40,46]. Due to the toughening effect of long-chain SPI, the over cross-linking of the tannin–sucrose adhesive system and the brittleness increase induced by water evaporation during hot pressing were relieved, and the degradation of bonding performance was avoided [47–49], macroscopically presenting good bonding strength and durability. Moreover, tannin and protein could bind to each other in the form of the combined action of multi-point hydrophobic bonds and hydrogen bonds, and the two could tanned into a compact tannin–protein spatial network cross-linking system, which could also contribute a lot to the bonding performance [50–52].

4. Conclusions

In this study, the whole-biomass tannin–sucrose–SPI adhesive was prepared and used in the preparation of plywood. When the SPI substitution ratio was 40%–50%, the viscosity of the composite adhesive was 4000 mPa·s, which could effectively avoid adhesive leakage. When SPI substitution rate was 40%, the bonding strength and stability of the adhesive were greatly improved. The boiling water bonding strength of tannin–sucrose–SPI adhesive reached 1.5 MPa (≥ 0.7 MPa, meeting the strength requirements of GB/T 17657-2013 Class I plywood), and the wood failure rate was up to 100%. Due to the large molecules and high reactivity of SPI, it compensated for the shortage of high temperature required for the conversion of sucrose into furanic cross-linker so that the tannin–sucrose–SPI adhesive experienced an efficient curing reaction at a low temperature of 190 °C, and the reaction degree and thermal stability of the curing product increased. The curing mechanism of the tannin–sucrose–SPI adhesive was very complicated, but it was certain that the conversion of sucrose into furan compounds, especially 5-HMF, was the core of the cross-linking reaction of the adhesive when elevating curing temperature. In addition, non-covalent interactions between SPI and tannin also contributed to the bonding strength. If this adhesive can further reduce the curing temperature, it has great practical application value and good promotion prospects in the fields of plywood, ecological boards, joinery boards, and other wood-based boards.

Author Contributions: Conceptualization, Z.W. and H.L.; methodology, G.X., J.L., Z.W. and H.L.; validation, G.X., J.L., F.G., W.G., Y.T. and D.L.; formal analysis, J.L., Z.W. and H.L.; investigation, G.X., J.L., F.G., W.G., Y.T. and D.L.; resources, G.X., J.L., F.G. and W.G.; writing—original draft preparation, G.X. and J.L.; writing—review and editing, G.X., J.L., Z.W. and H.L.; visualization, G.X., J.L., F.G., W.G., Y.T. and D.L.; supervision, J.L., Z.W. and H.L. All authors have read and agreed to the published version of the manuscript.

Funding: This research was funded by the National Natural Science Foundation of China (32160348 and 32160346), Department Program of Guizhou Province ([2020]1Y128), Forestry science and technology research project of Guizhou forestry bureau ([2020]C14), the Cultivation Project of Guizhou University of China ([2019]37).

Data Availability Statement: Not applicable.

Conflicts of Interest: The authors declare no conflict of interest.

References

1. Xu, C.; Xu, Y.; Chen, M.; Zhang, Y.; Li, J.; Gao, Q.; Shi, S.Q. Soy protein adhesive with bio-based epoxidized daidzein for high strength and mildew resistance. *Chem. Eng. J.* **2020**, *390*, 124622. [\[CrossRef\]](#)
2. Arbenz, A.; Avérous, L. Chemical modification of tannins to elaborate aromatic biobased macromolecular architectures. *Green Chemistry* **2015**, *17*, 2626–2646. [\[CrossRef\]](#)
3. Guigo, N.; Mija, A.; Vincent, L.; Sbirrazzuoli, N. Eco-friendly composite resins based on renewable biomass resources: Polyfurfuryl alcohol/lignin thermosets. *Eur. Polym. J.* **2010**, *46*, 1016–1023. [\[CrossRef\]](#)
4. Hussin, M.H.; Latif, N.; Hamidon, T.; Idris, N.; Hashim, R.; Appaturi, J.; Brosse, N.; Ziegler-Devin, I.; Chrusiel, L.; Fatriasari, W. Latest advancements in high-performance bio-based wood adhesives: A critical review. *J. Mater. Res. Technol.* **2022**, *21*, 3909–3946. [\[CrossRef\]](#)
5. Li, C.; Lei, H.; Wu, Z.; Xi, X.; Du, G.; Pizzi, A. Fully biobased adhesive from glucose and citric acid for plywood with high performance. *ACS Appl. Mater. Interfaces* **2022**, *14*, 23859–23867. [\[CrossRef\]](#)
6. Chen, X.; Yang, Z.; Yang, F.; Zhang, J.; Pizzi, A.; Essawy, H.; Du, G.; Zhou, X. Development of easy-handled, formaldehyde-free, high-bonding performance bio-sourced wood adhesives by co-reaction of furfuryl alcohol and wheat gluten protein. *Chem. Eng. J.* **2023**, *462*, 142161. [\[CrossRef\]](#)
7. Li, C.; Tang, Y.; Wang, Y.; Yuan, X.; Zhang, B.; Wu, Z.; Tian, H. A novel environmental-friendly adhesive based on recycling of *Broussonetia papyrifera* left forestry waste protein. *Forests* **2022**, *13*, 291. [\[CrossRef\]](#)
8. Xu, G.; Zhang, Q.; Xi, X.; Lei, H.; Cao, M.; Du, G.; Wu, Z. Tannin-based wood adhesive with good water resistance crosslinked by hexanediamine. *Int. J. Biol. Macromol.* **2023**, *234*, 123644. [\[CrossRef\]](#)
9. Gholami, M.; Shakeri, A.; Zolghadr, M.; Yamini, G. Non-isocyanate polyurethane from the extracted tannin of sumac leaves: Synthesis, characterization, and optimization of the reaction parameters. *Ind. Crop. Prod.* **2021**, *161*, 113195. [\[CrossRef\]](#)

10. Gonçalves, S.; Ferra, J.; Paiva, N.; Martins, J.; Carvalho, L.H.; Magalhães, F.D. Lignosulphonates as an Alternative to Non-Renewable Binders in Wood-Based Materials. *Polymers* **2021**, *13*, 4196. [[CrossRef](#)]
11. Siahkamari, M.; Emmanuel, S.; Hodge, D.B.; Nejad, M. Lignin-Glyoxal: A Fully Biobased Formaldehyde-Free Wood Adhesive for Interior Engineered Wood Products. *ACS Sustain. Chem. Eng.* **2022**, *10*, 3430–3441. [[CrossRef](#)]
12. Watcharakitti, J.; Win, E.E.; Nimnuan, J.; Smith, S.M. Modified Starch-Based Adhesives: A Review. *Polymers* **2022**, *14*, 2023. [[CrossRef](#)]
13. Maulana, M.I.; Lubis, M.A.R.; Febrianto, F.; Hua, L.S.; Iswanto, A.H.; Antov, P.; Kristak, L.; Mardawati, E.; Sari, R.K.; Zaini, L.H. Environmentally Friendly Starch-Based Adhesives for Bonding High-Performance Wood Composites: A Review. *Forests* **2022**, *13*, 1614. [[CrossRef](#)]
14. Din, Z.; Chen, L.; Xiong, H.; Wang, Z.; Ullah, I.; Lei, W.; Shi, D.; Alam, M.; Ullah, H.; Khan, S.A. Starch: An Undisputed Potential Candidate and Sustainable Resource for the Development of Wood Adhesive. *Starch Stärke* **2020**, *72*, 1900276. [[CrossRef](#)]
15. Pizzi, A.; Meikleham, N.; Stephanou, A. Induced accelerated autocondensation of polyflavonoid tannins for phenolic polycondensates. II: Cellulose effect and application. *J. Appl. Polym. Sci.* **1995**, *55*, 929–933. [[CrossRef](#)]
16. Meikleham, N.E.; Pizzi, A. Acid-catalyzed and alkali-catalyzed tannin-based rigid foams. *J. Appl. Polym. Sci.* **1994**, *53*, 1547–1556. [[CrossRef](#)]
17. Rossouw, D. Reaction Kinetics of Phenols and Tannin with Aldehydes. Ph.D. Thesis, University of South Africa, Gauteng, South Africa, 1979.
18. Boran, S.; Usta, M.; Ondaral, S.; Gümüşkaya, E. The efficiency of tannin as a formaldehyde scavenger chemical in medium density fiberboard. *Compos. Part B* **2012**, *43*, 2487–2491. [[CrossRef](#)]
19. Bisanda, E.; Ogola, W.; Tesha, J. Characterisation of tannin resin blends for particle board applications. *Cement Concrete Comp.* **2003**, *25*, 593–598. [[CrossRef](#)]
20. Liu, S.; Yang, H.; Ran, X.; Yang, L.; Du, G. Synthesis, structure and performance of pulp-based wood adhesives. *J. For. Eng.* **2022**, *7*, 132–139.
21. Grigsby, W.; Warnes, J. Potential of tannin extracts as resorcinol replacements in cold cure thermoset adhesives. *Holz RohWerkst.* **2004**, *62*, 433–438. [[CrossRef](#)]
22. Casanova, M.; Morgan, K.T.; Gross, E.A.; Moss, O.R.; Heck, H.D. DNA-protein cross-links and cell replication at specific sites in the nose of F344 rats exposed subchronically to formaldehyde. *Fundam. Appl. Toxicol.* **1994**, *23*, 525–536. [[CrossRef](#)]
23. Liang, J.; Wu, Z.; Xi, X.; Lei, H.; Zhang, B.; Du, G. Investigation of the reaction between a soy-based protein model compound and formaldehyde. *Wood Sci. Technol.* **2019**, *53*, 1061–1077. [[CrossRef](#)]
24. Xi, X.; Pizzi, A.; Frihart, C.R.; Lorenz, L.; Gerardin, C. Tannin plywood bioadhesives with non-volatile aldehydes generation by specific oxidation of mono- and disaccharides. *Inter. J. Adhes. Adhes.* **2020**, *98*, 102499. [[CrossRef](#)]
25. Li, K.; Geng, X.; Simonsen, J.; Karchesy, J. Novel wood adhesives from condensed tannins and polyethylenimine. *Int. J. Adhes. Adhes.* **2004**, *24*, 327–333. [[CrossRef](#)]
26. Sun, G.; Sun, H.; Liu, Y.; Zhao, B.; Zhu, N.; Hu, K. Comparative study on the curing kinetics and mechanism of a lignin-based epoxy/anhydride resin system. *Polymer* **2007**, *48*, 330–337. [[CrossRef](#)]
27. Ghahri, S.; Pizzi, A. Improving soy-based adhesives for wood particleboard by tannins addition. *Wood Sci. Technol.* **2018**, *52*, 261–279. [[CrossRef](#)]
28. Pizzi, A. Wood products and green chemistry. *Ann. For. Sci.* **2016**, *73*, 185–203. [[CrossRef](#)]
29. Xiao, G.; Liang, J.; Li, D.; Tu, Y.; Zhang, B.; Gong, F.; Gu, W.; Tang, M.; Ding, X.; Wu, Z. Fully bio-based adhesive from tannin and sucrose for plywood manufacturing with high performances. *Materials* **2022**, *15*, 8725. [[CrossRef](#)]
30. Zhao, S.; Wang, Z.; Li, Z.; Li, L.; Li, J.; Zhang, S. Core-shell nanohybrid elastomer based on co-deposition strategy to improve performance of soy protein adhesive. *ACS Appl. Mater. Inter.* **2019**, *11*, 32414–32422. [[CrossRef](#)]
31. Wu, Z.; Xi, X.; Lei, H.; Liang, J.; Liao, J.; Du, G. Study on soy-based adhesives enhanced by phenol formaldehyde cross-linker. *Polymers* **2019**, *11*, 365. [[CrossRef](#)]
32. Wu, Z.; Liang, J.; Lei, H.; Zhang, B.; Xi, X.; Li, L. Study on soy protein-based adhesive cross-linked by glyoxal. *J. Renew. Mater.* **2021**, *9*, 205–218. [[CrossRef](#)]
33. Li, C. Preparation and Application on Research of Chemical Crosslinking Modification of Soy Bean Meal-Based Adhesive. Ph.D. Thesis, Beijing Forestry University, Beijing, China, 2015.
34. GB/T 17657-2022; Test Method for Physical and Chemical Properties of Wood-Based Panels and Veneer Panels. Standards Press: Beijing, China, 2022.
35. Kaspchak, E.; Goedert, A.; Mafra, L.; Mafra, M. Effect of divalent cations on bovine serum albumin (BSA) and tannic acid interaction and its influence on turbidity and in vitro protein digestibility. *Int. J. Biol. Macromol.* **2019**, *136*, 486–492. [[CrossRef](#)] [[PubMed](#)]
36. Wu, Z. Crosslinking Modification of Protein-Based Adhesives and Mechanism. Ph.D. Thesis, Beijing Forestry University, Beijing, China, 2016.
37. Wu, Z.; Xi, X.; Lei, H.; Du, G.; Zhang, B.; Wang, X.; Wang, H. Modification of tannin-soy based adhesive coordination with plasma in plywood. *J. Southwest For. Univ.* **2017**, *37*, 199–205.
38. Lei, H.; Wu, Z.; Cao, M.; Du, G. Study on the soy protein-based wood adhesive modified by hydroxymethyl phenol. *Polymers* **2016**, *8*, 256–265. [[CrossRef](#)]

39. Chen, J.; Chen, X.; Zhu, Q.; Chen, F.; Zhao, X.; Ao, Q. Determination of the domain structure of the 7S and 11S globulins from soy proteins by XRD and FTIR. *J. Sci. Food Agric.* **2013**, *93*, 1687–1691. [[CrossRef](#)]
40. Deng, X.; Wu, Z.; Zhang, B.; Lei, H.; Liang, J.; Li, L.; Tu, Y.; Li, D.; Xiao, G. A new wood adhesive based on recycling *Camellia oleifera* cake-protein: Preparation and properties. *Materials* **2022**, *15*, 1659. [[CrossRef](#)]
41. Seino, H.; Uchibori, T.; Nishitani, T.; Inamasu, S. Enzymatic synthesis of carbohydrate esters of fatty acid (I) esterification of sucrose, glucose, fructose and sorbitol. *JAOCS* **1984**, *61*, 1761–1765. [[CrossRef](#)]
42. Zhao, Z.; Umemura, K. Investigation of a new natural particleboard adhesive composed of tannin and sucrose. *J. Wood Sci.* **2014**, *60*, 269–277. [[CrossRef](#)]
43. Zhao, Z.; Umemura, K. Investigation of a new natural particleboard adhesive composed of tannin and sucrose. 2. Effect of pressing temperature and time on board properties, and characterization of adhesive. *Bioresources* **2015**, *10*, 2444–2460. [[CrossRef](#)]
44. Zhao, H.; Holladay, J.E.; Brown, H.; Zhang, Z.C. Metal chlorides in ionic liquid solvents convert sugars to 5-hydroxymethylfurfural. *Science* **2007**, *316*, 1597–1600. [[CrossRef](#)]
45. Munshi, M.; Lomate, S.; Deshpande, R.; Rane, V.; Kelkar, A. Synthesis of acrolein by gas-phase dehydration of glycerol over silica supported Bronsted acidic ionic liquid catalysts. *J. Chem. Technol. Biot.* **2010**, *85*, 1319–1324. [[CrossRef](#)]
46. Sun, S.; Zhao, Z.; Umemura, K. Further exploration of sucrose-citric acid adhesive: Synthesis and application on plywood. *Polymers* **2019**, *11*, 1875. [[CrossRef](#)] [[PubMed](#)]
47. Kan, H.; Kan, Y.; He, W.; Gao, Z. Effects of pH value of water-based polymer on properties of a polyamide-based API adhesive. *J. For. Eng.* **2023**, *8*, 87–94.
48. Li, C.; Ye, H.; Ge, S.; Yao, Y.; Ashok, B.; Hariram, N.; Liu, H.; Tian, H.; He, Y.; Guo, G.; et al. Fabrication and properties of antimicrobial flexible nanocomposite polyurethane foams with in situ generated copper nanoparticles. *J. Mater. Res. Technol.* **2022**, *19*, 3603–3615. [[CrossRef](#)]
49. Yang, F.; Jin, C.; Wang, S.; Wang, Y.; Wei, L.; Zheng, L.; Gu, H.; Lam, S.; Naushad, M.; Li, C.; et al. Bamboo-based magnetic activated carbon for efficient removal of sulfadiazine: Application and adsorption mechanism. *Chemosphere* **2023**, *323*, e138245. [[CrossRef](#)]
50. Zhao, Y.; Zhai, Y.; Xu, Y.; Zhang, L.; Wang, Z. Polymerization and product characteristics of polyphenols of *Pinus sylvestris* var. mongolicabarks and protein. *J. Beijing For. Univ.* **2016**, *38*, 102–107.
51. Peng, J.; Yan, C.; Yang, F.; Hong, M.; Yang, Z.; Du, G.; Zhou, X. Preparation of tannin-urea-formaldehyde resin by carbonated tannin and its bonding properties. *J. For. Eng.* **2023**, *8*, 119–125.
52. Li, H.; Wang, Y.; Xie, W.; Tang, Y.; Yang, F.; Gong, C.; Wang, C.; Li, X.; Li, C. Preparation and characterization of soybean protein adhesives modified with an environmental-friendly tannin-based resin. *Polymers* **2023**, *15*, 2289. [[CrossRef](#)]

Disclaimer/Publisher’s Note: The statements, opinions and data contained in all publications are solely those of the individual author(s) and contributor(s) and not of MDPI and/or the editor(s). MDPI and/or the editor(s) disclaim responsibility for any injury to people or property resulting from any ideas, methods, instructions or products referred to in the content.